URN (Paper): urn:nbn:de:gbv:ilm1-2014iwk-058:8

58th ILMENAU SCIENTIFIC COLLOQUIUM
Technische Universität Ilmenau, 08 – 12 September 2014
URN: urn:nbn:de:gbv:ilm1-2014iwk:3

INTERFEROMETRICAL DETERMINATION OF CONCENTRIC RUN-OUT ERRORS IN ROTARY TABLES FOR OPTICAL ROUNDNESS MEASUREMENT

Vinzenz Ullmann, Michael Kühnel, Eberhard Manske

Technische Universität Ilmenau, Institute for Process Measurement and Sensor Technology

ABSTRACT

For high-accuracy roundness measurements of ring gauges it is necessary to know the uncertainty input of the parasite influences to the recorded data. The experience in roundness measurements showed that one of the largest deviations is caused by the concentric run-out error of the utilized rotary table. A novel optical probe head basing on laser interferometers has a measurement resolution up to 20 pm to detect a relative change in length. Hence, it is a promising experiment to use this optical probe head technology for the concentric run-out detection. It is possible to show the accuracy potential in interferometrical form measurements of ring gauges. Therefore, the institute for process measurement and sensor technology developed an optical principle based on established and adapted measurement methods in concentric run-out error detection. The main goal is to increase the reproducibility of the whole measurement system by using the interferometrical sensor technologies for recording a table specific concentric run-out error. After that it is possible to correct the roundness measurement results in the future by subtraction of the recorded data from the roundness measurement data. This publication presents measurement results for the concentric run-out error of a system-integrated rotary table which includes air bearings. The investigations of this table show a maximal concentric run-out error of 537.51 nm. It was possible to determine this error with a reproducibility of 31.31 nm in maximum.

Keywords **–** Roundness measurement, laser interferometry, concentric run-out error, non-tactile, rotary tables

1. INTRODUCTION

In the last years one of the research fields at the Institute for Process Measurement and Sensor Technology (IPMS) was the development and investigation of systems for optical roundness measurement. Sensor technology basing on interferometers has the ability to increase the accuracy and to decrease the duration of roundness measurements [1], [2], [3]. Furthermore, in optical test principles there are no manipulations on measuring object surface like physical or chemical abrasions [4]. In addition to that the probe head interacts without any force input to the measuring object during the whole scanning process. In this case it can be guaranteed that the measuring object has the same geometrical characteristics after the scanning like before. This advantage is transferable for roundness and cylindrical shape determination on ring gauges utilizing laser interferometers.

Basically, a roundness measurement is carried out by rotating the workpiece with help of a rotary table and measuring its radius variation. Therefore the measured signal not only comprises the roundness deviation of the workpiece but also misalignment errors with respect to the rotary axis and run-out errors of the rotary table. The first, the ring alignment, contains two position aberrations compared to the rotary table axis. An automated adjustment reduces

the absolute deviation of the ring eccentricity and the ring tilt. Additionally, mathematical compensation algorithms decrease the uncertainty part of position errors in the measurement results. For a correct roundness measurement it is necessary to know the accurate dynamic characteristics of the rotary table. Each roundness measurement system which is equipped with tactile or with optical sensors requires the concentric run-out error of the utilized rotary table as dataset to achieve a low uncertainty in measurements. The data processing requires a separation of this concentric run-out error from the ring gauge values. Hence, for an exact measurement with a decreased uncertainty it is necessary to record the concentric run-out error with highest precision. To investigate this error with an optical technology the interferometrical roundness measurement setup with two laser interferometers was tested.

2. MEASUREMENT SETUP

The basic measurement principle is the interferometrical detection of small length differences (nm-range) relative to a defined rotary axis. This axis is defined by a utilized rotary table which has a concentric run-out error. The ring gauge is on the top of this table. Two laser interferometers measure the radius in dependence of the rotary table axis angle in two index arms (figure 1). The main concept of this non-tactile measurement system is the direct optical touch between the interferometer beam and the technical surface of the ring gauge. Therefore, the probe head construction with two laser interferometers allows the optical scanning of ring gauge surfaces at two positions simultaneously. A beam guiding system controls the scanning positions and the 180 degree angle offset between the first and the second laser beam. The laser beams are guided to the ring surface by the use of two 90° prisms which are arranged in the middle axis of the probe head.

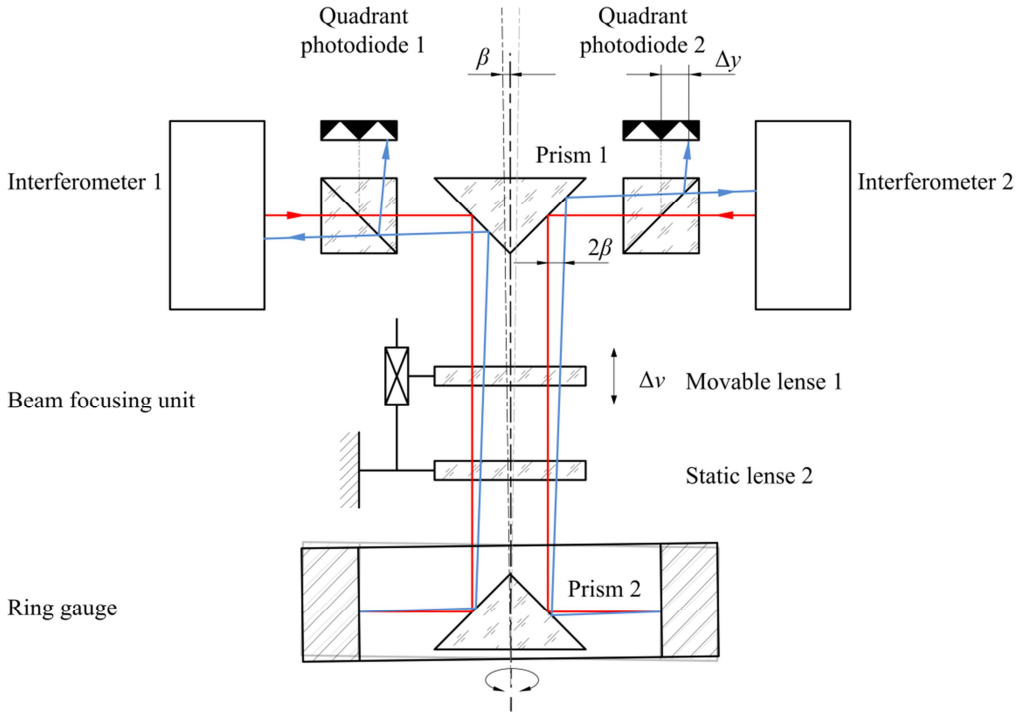

Figure 1: Probe head principle based on two laser interferometers – tilting effects during the measurement process and their detection

Due to the cylindrical shape of the ring gauge, the beams have to be focused on the cylindrical surface to reduce a distortion of the reflected beams. Different ring diameters require a different focal length. An adaptive optical system forms the wave fronts for a direct

measuring at the cylindrical surface of the ring gauges. This focusing unit contains a movable and a static cylindrical lens. It can be used for ring diameters in a range between 10 mm and 300 mm.
Figure 2 shows the realized measuring setup in laboratory. This is the same system which was described by Kühnel in 2011 [2] but it includes some additional or enhanced construction elements which are developed by the optimization processes of the last three years.

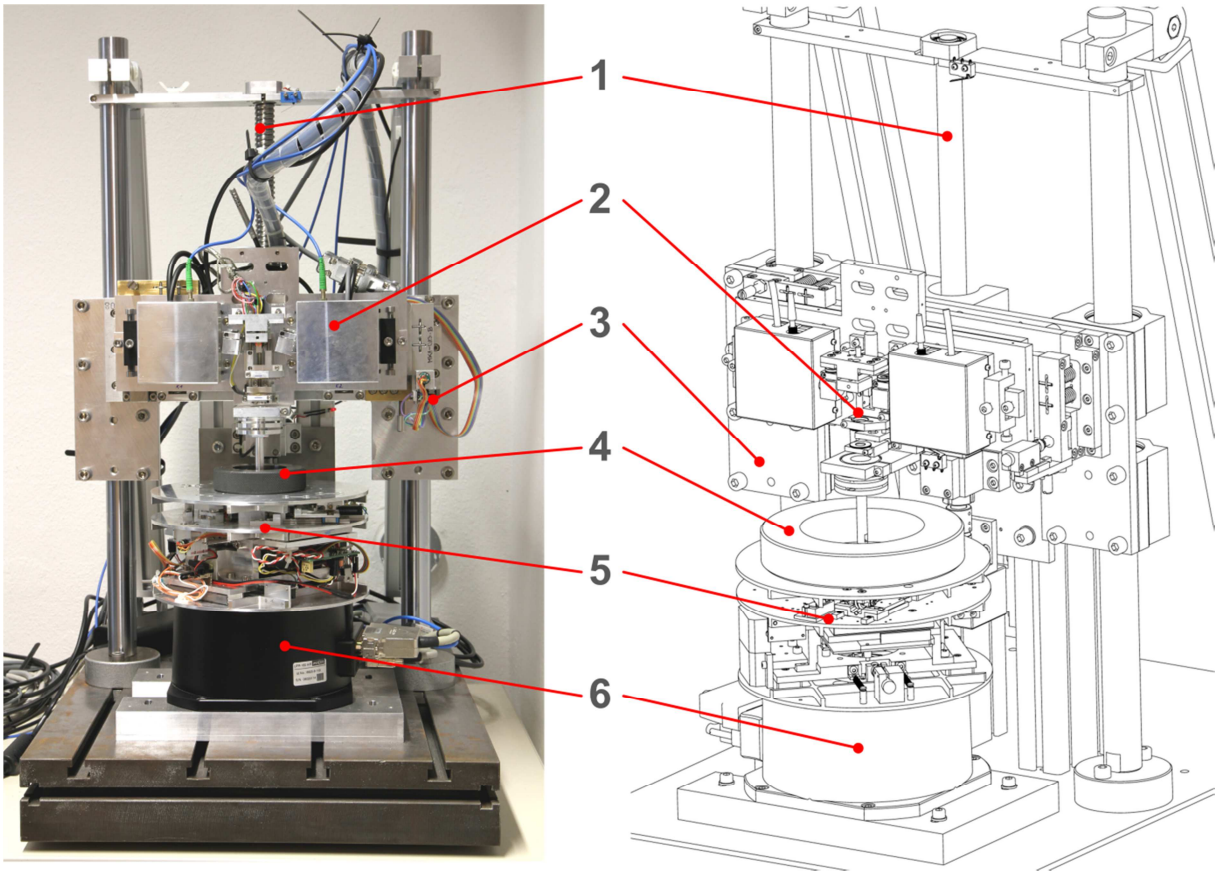

Figure 2: Realized measurement setup including: 1-spindle for z-axis adjustment, 2-probe head with two interferometers, 3-portal with probe head adjusting elements, 4-Ring gauge, 5-Stage for x- and y-axis alignment, 6-Tested rotary table with air bearings

Furthermore, the whole measuring system contains a portal for the probe head, a PC-controlled data acquisition module with an integrated laser unit as well as a complete positioning stage for the tested rotary table. The portal contains a spindle drive for an additional cylinder shape determination in the measuring mode.

3. MEASUREMENT METHOD

3.1 Measurement preparation and ring gauge alignment

Before the measuring process of the concentric run-out error starts, the positioning stage of the rotary table moves and tilts the deposited ring gauge to overlap the ring middle axis with the rotary axis to compensate the influences of the ring tilting and the ring eccentricity. In addition to that an alignment process is necessary to get useable interferometer signals. This circumstance requires laser beams which reflect nearly 180° back in the direction to the interferometers. Therefore, an automated alignment process measures the tilting angle β and the eccentricity $e(\alpha)$ of the ring gauge position. Two beam splitters divide the reflected laser beams and guide one part to a quadrant photodiode for the angles (α,β) detection. The second

part passes the beam splitter and enters the interferometer (figure 1 including tilt angle β). In case of the tilt angle detection β is calculated with equation 3.1.

$$\beta = \frac{1}{2} \cdot \arctan\left(\frac{\Delta y}{L}\right) \tag{3.1}$$

Hence, the beam offset Δy depends on the tilt angle β. The beam length L is the optical path between the ring surface and the quadrant photodiode. The eccentricity depended beam alignment is shown in figure 3.

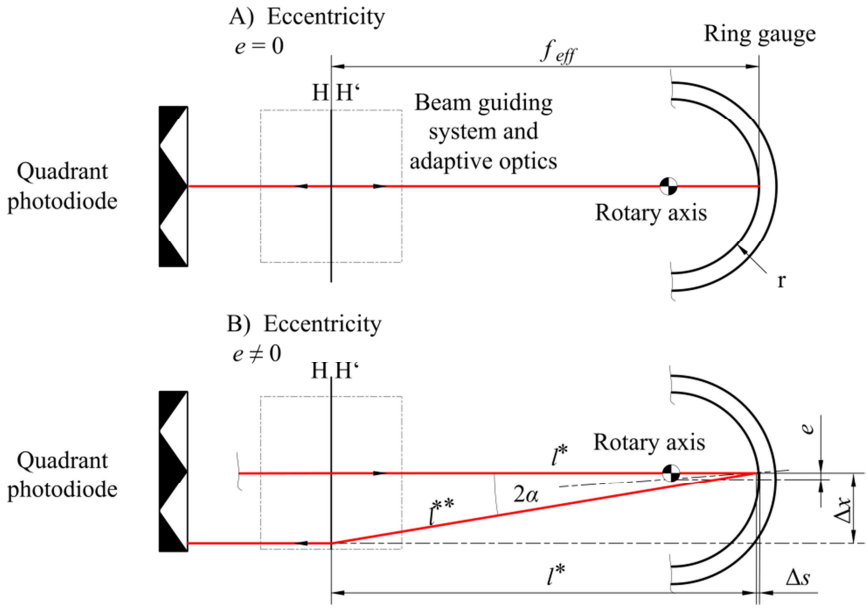

Figure 3: Eccentricity determination with the quadrant photodiode

$$e_{det} \approx r \cdot tan\left[\frac{1}{2} \cdot arctan\left(\frac{\Delta x}{f_{eff}}\right)\right], e \ll r \rightarrow \Delta s \approx 0,\ f_{eff} = l^* \tag{3.2}$$

The aligned beam angles 2α and 2β between the incoming and reflected beams have to be smaller than 0.5° [1] for a valid photodiode signal. This is realizable with a manual adjusting. For a valid interferometer signal the angles have to be smaller than one angle minute. This is realizable with the automatic alignment process which uses the quadrant photodiode signals.
Now with an available interferometer signal it is possible to detect the eccentricity by the calculation of the sum and the difference signal of both index arm signals with a nanometer resolution. Due to that, the difference signal $D(\varphi, \gamma)$ (equation 3.4) delivers the fourfold eccentricity (e) and the sum signal $S(\varphi, \gamma)$ (equation 3.5) compresses the influence of the eccentricity in the measurement signal. S_{max} is the diameter deviation of the ring gauge. The angle φ is the measurement position and the angle γ is the direction of the eccentricity. The relationship is given in equation 3.2 and in figure 4.

$$\rho(\varphi) = w(\varphi) - r = e \cdot cos(\varphi - \gamma) + \sqrt{r^2 - e^2 \cdot \sin^2(\varphi - \gamma)} - r \tag{3.3}$$

$$D(\varphi) = \rho(\varphi) - \rho(\varphi + 180°) = 2 \cdot e \cdot \cos(\varphi - \gamma) \tag{3.4}$$

[1] The angle value depends on the ring gauge diameter, in this case the ring diameter is 100mm

$$S(\varphi) = \rho(\varphi) + \rho(\varphi + 180°) = 2 \cdot \left[\sqrt{r^2 - e^2 \cdot \sin^2(\varphi - \gamma)} - r\right] \tag{3.5}$$

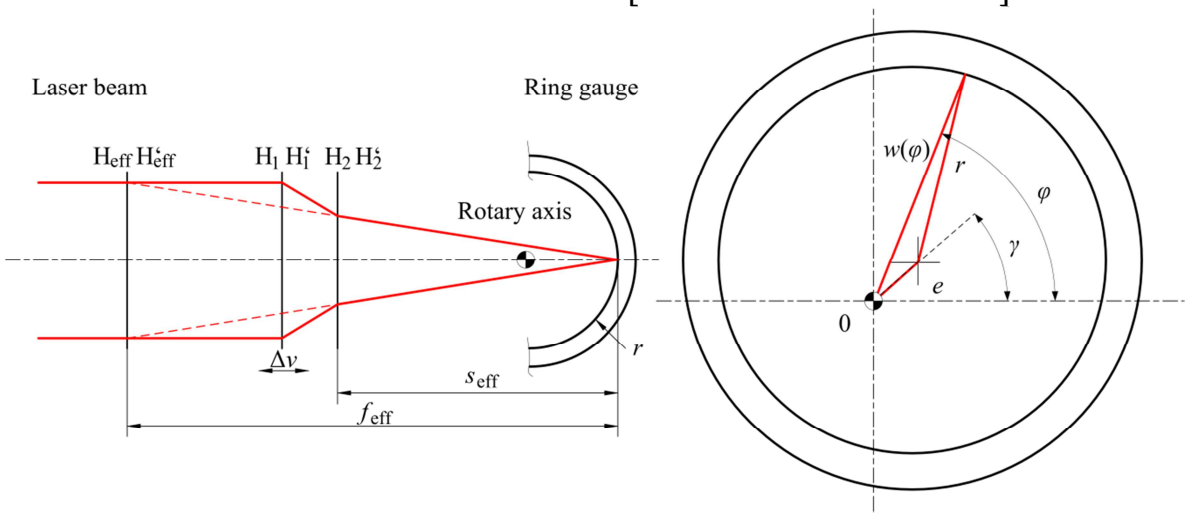

Figure 4: Principle of the zoom lens system (left) and principle of roundness measurement in one index arm

The lowest achievable eccentricity is less than 0.1 µm and limited by the resolution of the positioning stage. After the alignment process with a whole duration of less than 120 s the eccentricity of the ring gauge is between one and two micrometers. That is an adequate eccentricity for usable interferometer signals. The reason for this remaining eccentricity is a stick-slip effect in the linear guiding systems of the x-y-alignment stage. Hence, it is necessary to subtract the eccentricity in the following data processing step.

3.2 Measurement data acquisition and data processing

In every new data acquisition the number of sampled values in each roundness measurement step over an area of 360° is n=9000. The sampling time respectively the measurement time is t=30 s. The measurement is triggered by the own incremental position sensor of the rotary table. An additional electronic device converts the sinusoidal signal of this sensor in a TTL-compatible rectangular signal which is used for the start and stop trigger of the interferometer data acquisition module.

It is necessary to use a data processing before the calculation of the concentric run-out error can start. For example the residual eccentricity (see 3.1) has to be subtracted from the roundness values. But there are some other systematical errors which have to be corrected. The most important in the interferometrical setup are determined and compared at the institute. Table 1 includes these results [5].

Table 1: Systematical error values a measured roundness [5] of a 60mm ring gauge in three sections

Systematical error	Determined divergence ΔR (Min…Max)	Correction method
Linear signal drift	0.009 µm…0.016 nm	Linear drift correction
Surface roughness and signal noise	0.061 µm…0.123 µm	Mean value filter + low-pass filter
Eccentricity	0.63 µm…1.993 µm	Harmonic analysis
Concentric run-out error	0.54 µm	Subtraction from roundness data

The smallest influence is given by the linear signal drift of the interferometers during the measurement sampling. To correct this error the difference between the first mean value of

the last five values and the second mean value of the first five values in the roundness data generates a slope (a) if this difference gets divided by the number of values in the measured data (n); i is the array index:

$$a = \frac{\left(\frac{\left(\sum_{i=0}^{4} x_{[n-(i+1)]}\right)}{5} - \frac{\left(\sum_{i=0}^{4} x_i\right)}{5}\right)}{n} \tag{3.6}$$

After that the all values in the measured array can be corrected by subtraction of the product between their index (i) and the slope (a):

$$d(x_i) = x_i - a \cdot i \tag{3.7}$$

The surface roughness and the signal noise are reduced by using a mean value filter over nine nearby values in combination with an additional low-pass filter. The low-pass filter is designed by the rules which are given in DIN EN ISO 12181-2 [6] and in VDI/VDE 2631 [7]. But caused by the optical instead of tactile interaction between the probe head and the object surface it is not possible to transfer all rules in detail to the data processing of optical measurement data. For example in our measurement setup there is no stylus head diameter. The designed low-pass filter has its cut-off wavenumber now at 150 W/U.
The eccentricity can be calculated with a harmonic analysis [8] of the first order in every roundness measurement data array.

$$a = \frac{2}{n} \cdot \sum_{i=0}^{n-1} x_i \cdot \cos\psi_i = \Delta x_e \tag{3.8}$$

$$b = \frac{2}{n} \cdot \sum_{i=0}^{n-1} x_i \cdot \sin\psi_i = \Delta y_e \tag{3.9}$$

With both coefficients it is possible to calculate the eccentricity e and the phase φ angle. After that the next data processing step subtracts the eccentricity from the measured data array.

3.3 Calculation of the concentric run-out error

The tested rotary table with air bearings is investigated by the Donaldson reversal method [9], [10]. Therefore the system measures the workpiece two times, but before the second measurement the ring is manually rotated by 180 degree with respect to the table and new automatically adjusted before (see the section 3.1). Both measurements determine the ring and the concentric run-out error twice with two interferometers, but in the second measurement with an angle phase difference of 180 degree (compare with figure 5) of the ring gauge roundness.
After the data processing step (section 3.2) it is possible to calculate the two run-out errors (L_1, L_2) and a mean value of both with these four datasets (cross-over subtraction (1), (2)).

$$L_1 = \frac{I_{1,0°} - I_{2,180°}}{2} \tag{3.10}$$

$$L_2 = \frac{I_{1,180°} - I_{2,0°}}{2} \tag{3.11}$$

$I_{1,0°}$ is the measured data array of the first interferometer with the ring gauge in 0° position and $I_{2,180°}$ is the array of the second interferometer after the changed ring position. The advantage of two utilized interferometers allows that there is no need to rotate the probe head together with ring. This circumstance increases the measurement speed. All of the following measurements are processed in the quality control laboratory of LMW Schmalkalden GmbH. The laboratory room has controlled environmental conditions with a stabilized temperature of 20 °C. This circumstance helps by controlling the environmental influences to the refraction index in air and the resulting influences to the interferometer signals.

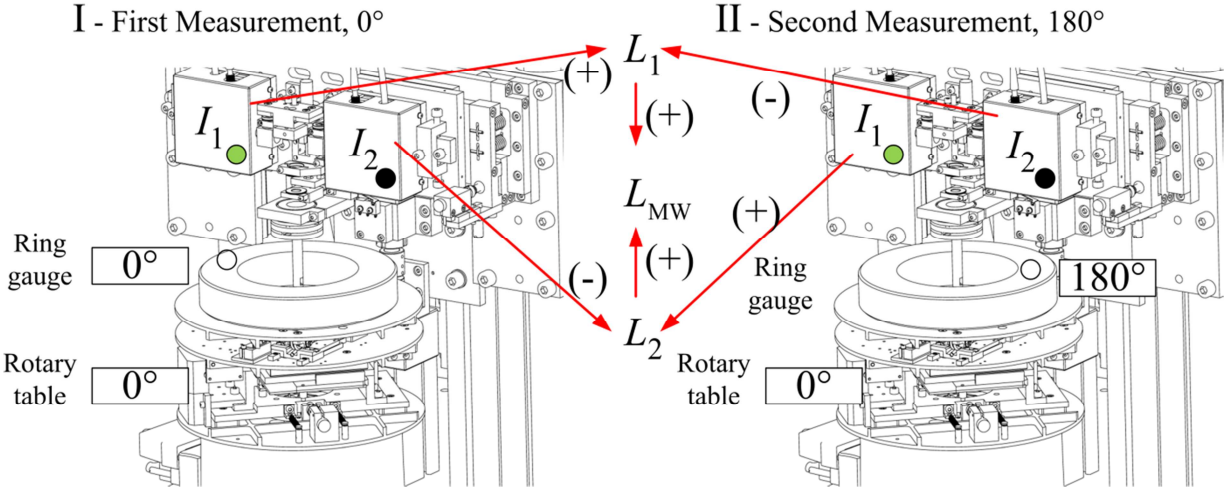

Figure 5: Start/End points of the two measurements for concentric run-out detection with Donaldson reversal method

4. MEASUREMENT RESULTS

4.1 Determined concentric run-out error

In experiments the concentric run-out error of the used rotary table PI MICOS UPR-160 AIR was determined. Its spindle error has a periodic 360 degree characteristic. This is caused by the implemented air bearings instead of ball bearings (720 degree characteristic). Hence, after one rotation the same error gradient repeats. The complete concentric run-out error is diagramed in figure 6.

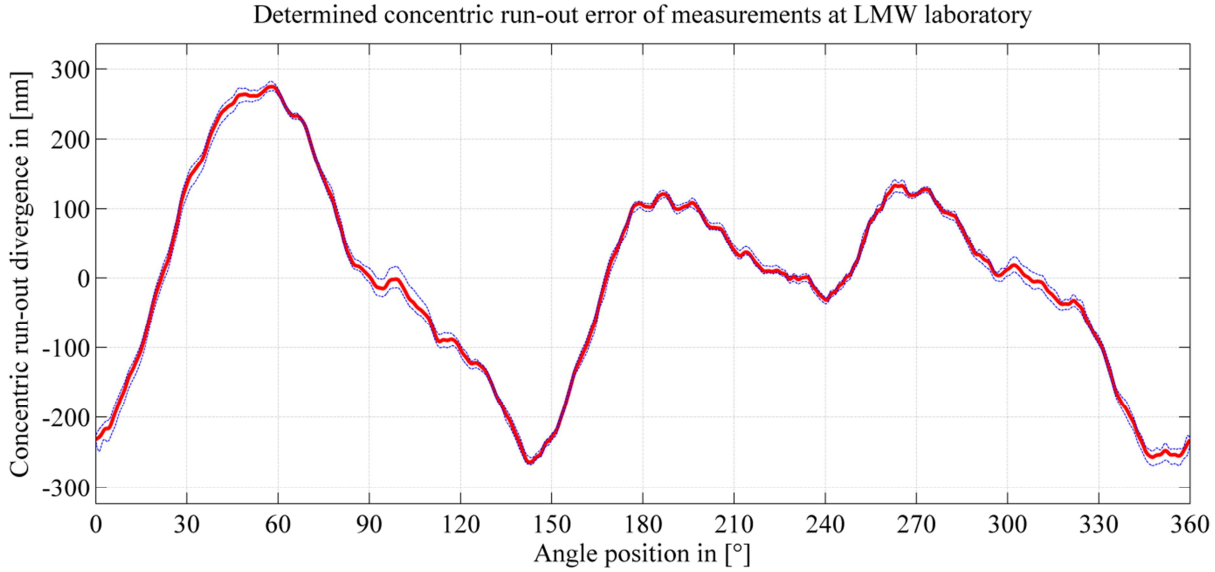

Figure 6: Mean concentric run-out error of the used rotary table MICOS UPR-160 AIR over all concentric run-out measurements; the grey dotted lines represent the variance limits of the concentric run-out error

It is the mean value of the measured error with different ring gauge diameters of 20 mm, 40 mm, 50 mm and 60 mm. The curve is normed to the mean value of all sampling points. The peak-to-peak divergence is 537.51 nm. There are two additional dotted lines in the diagram in figure 6. They show the variance limits which are generated by all measured mean values of the concentric run-out error. This gives a first outlook to the reproducibility results which are discussed in section 4.2.

4.2 Reproducibility tests

Four series of measurement generates four curves (figure 7) for concentric run-out errors of the investigated rotary table. The intention for the choice of the used ring gauge diameters was to investigate correlations between the mass of the ring gauges, their diameter and the resulting measurement reproducibility. Thus, the result measurements show no dependencies to different masses.

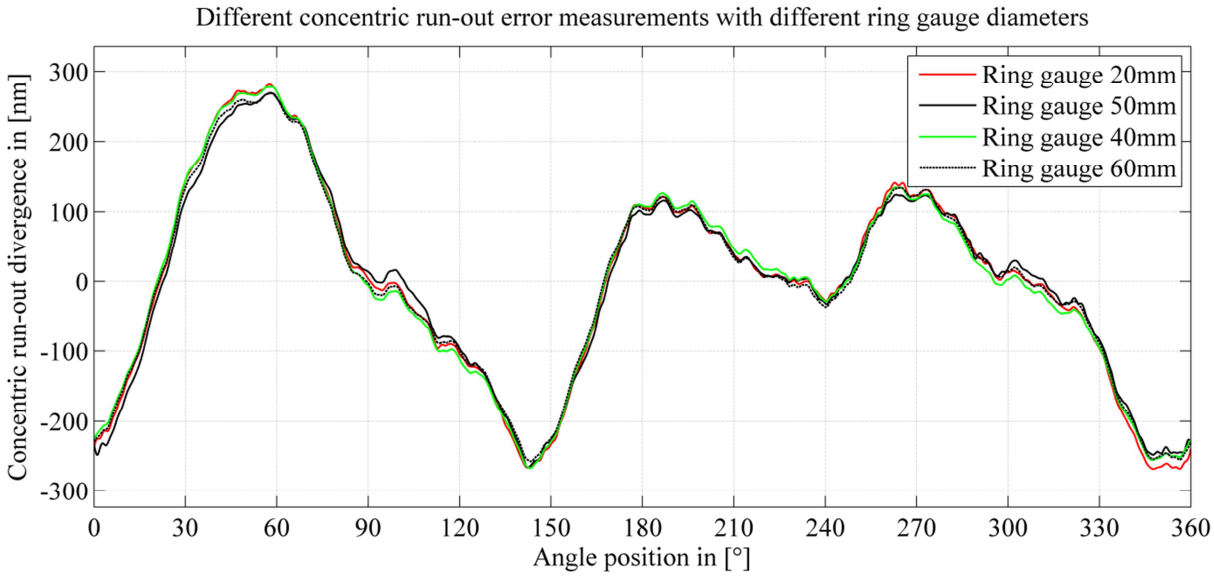

Figure 7: Concentric run-out errors for the tested rotary table MICOS UPR-160 determined with four different ring gauge diameters

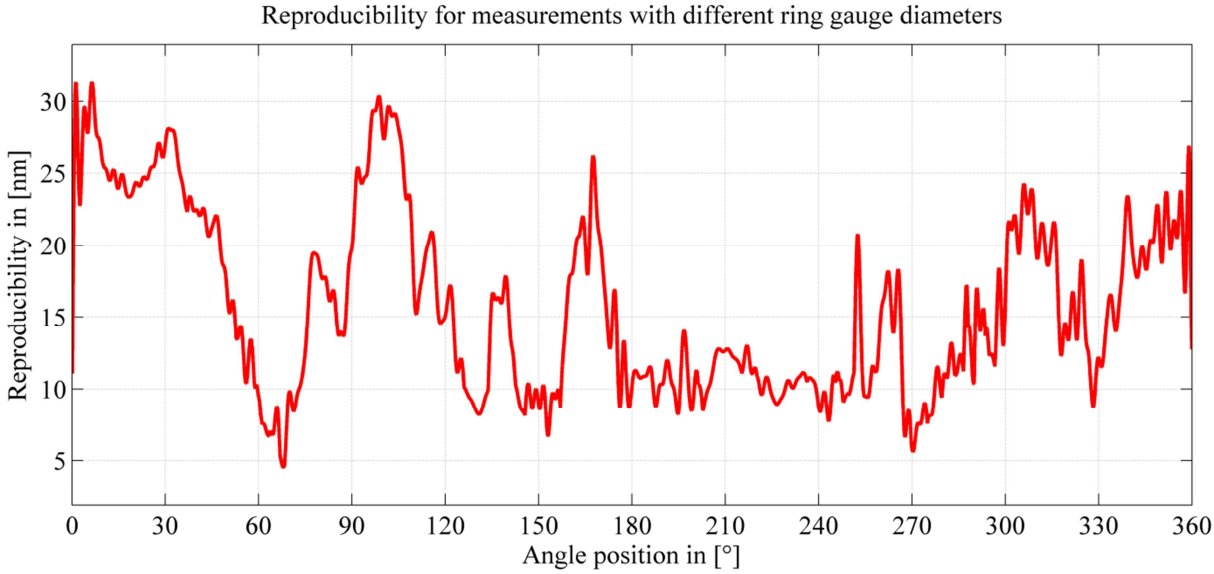

Figure 8: Reproducibility for compared measurements with the following ring gauge diameters: 20mm, 40mm, 50mm and 60mm

In addition to that there is a long time gap of five months between the measurements of the 20 mm and 50 mm gauges and the measurements of the 40 mm and 60 mm gauges. This circumstance shows a high long-term stability of the measurement setup.
Figure 8 shows the maximum divergence in each sampling point of all four determined ring gauge concentric run-out errors. It is interesting to see that there are graph sections with an increased reproducibility of the concentric run-out error. This indicates an inhomogeneity of the spindle axis position stability over the 360° of the rotary table, but measurements with honed gauges instead of lapped gauges show a correlation between the reproducibility and the surface character (see section 4.3). A superposition of both effects is conceivable, too. The calculated mean reproducibility is 15.83 nm. But the maximum divergence for the concentric run-out determination with different ring gauges is 31.31 nm. The minimum divergence of 4.53 nm shows the high metrological potential of the optical measurement setup.

4.3 Investigation of systematical correlations

There was the possibility for an investigation and comparison of the reproducibility between honed and lapped ring gauges. Figure 9 includes the reproducibility for two series of measurements which consists ten single measurements of the concentric run-out errors.

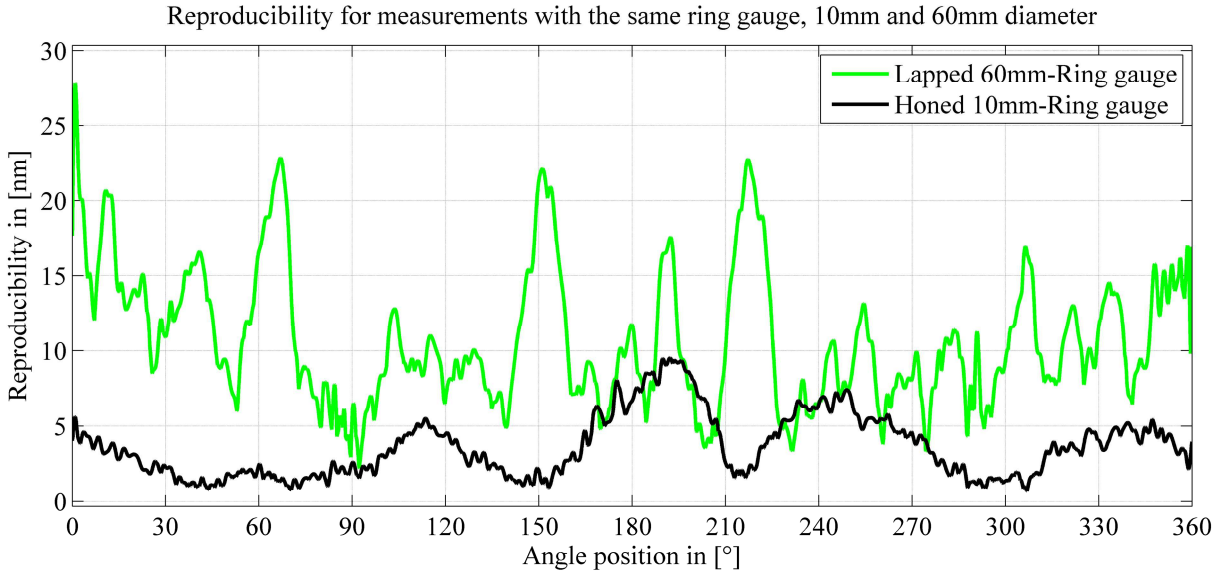

Figure 9: Comparison of the reproducibility between measurements with honed ring gauges and lapped ring gauges

The mean reproducibility is 3.63 nm between the maximum divergence of 9.51 nm and the minimum divergence of 0.70 nm for the 10 mm ring gauge. This ring gauge has a honed surface. For the 60 mm ring gauge with a lapped surface the mean reproducibility is 10.75 nm between the maximum divergence of 27.79 nm and the minimum divergence of 2.23 nm. Hence, the measurement accuracy with honed ring gauges is nearly three times higher than using lapped ring gauges with this optical measurement setup. This is an unexpected result because the honed surfaces have an increased roughness. Though the surface roughness decreases the signal quality of the laser interferometers but there are no dominating scrapers at the surface like on lapped ring gauges which have a large influences to the length signal by an additional beam tilting.
Another investigation aspect is the tilting of the rotary table which results in different concentric run-out errors for different measuring sections. The results for comparing measurement in different ring gauge heights are shown in figure 10. The first height is measured two millimeters above the ring gauge bottom and the second height is measured two

millimeters below the top of the ring gauge. The peak-to-peak divergence between both concentric run-out errors is 53.91 nm for the 40 mm ring gauge and 42.26 nm for the 60 mm ring gauge and these values are higher than the determined reproducibility. Hence, the concentric run-out error is changing by measuring in different heights. The reason for this is a wobbling of the rotary table. Thus, measurements in different sections require their own determined concentric run-out error to compensate the influence in roundness measurements.

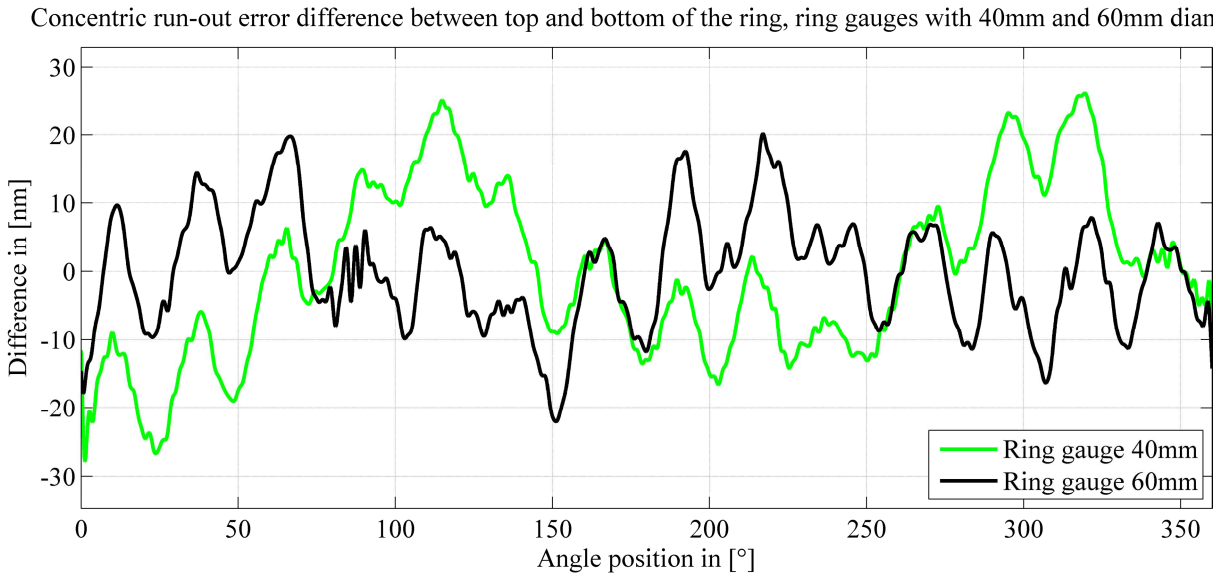

Figure 10: Comparison between two ring gauge concentric run-out errors which are measured in different heights.

5. CONCLUSIONS

In result the special construction of the probe head and the two utilized Michelson interferometers support the determination of concentric run-out errors with highest accuracy. The concentric run-out error including the axis eccentricity error and axis wobbling error in the work level of the whole roundness measurement system is determined with 537.51 nm in maximum during the 360°-rotation. The reproducibility of these measurements is 31.31 nm in maximum and 4.53 nm in minimum. Reproducibility tests in a series of measurements with one ring gauge shows differences between honed and lapped ring gauges. It seems that the honed ring surface is an advantage for this kind of optical measurements. The reproducibility with the honed ring gauge is between 0.70 nm and 9.51 nm for each of the 9000 sampling points in ten single measurements. The reproducibility with the lapped ring gauge is between 2.23 nm and 27.79 nm. Further investigations with honed ring gauges are required to confirm this assumption that the honed surface increases the reproducibility in the optical measurement. In conclusion the results have shown that the optical system is not only qualified for highest accuracy standards in roundness measurements [1] but also in run-out error measurements with an additional acquisition of measurement speed.

6. OUTLOOK

The setup will be tested in the future with more and different measuring objects. It is planned to realize system optimizations. The goal is to get lower uncertainties for the roundness and cylinder form measurements with this measuring system. More measurements of the concentric run-out error will help to increase the data base for the compensation of it in roundness measurements. Hence, it will be possible to correct the measurement values of

different ring gauges with a higher accuracy by respect to their considered weight and surface character. In addition to that the information about the adjustment stability in the optical system will be assured.

7. ACKNOWLEDGMENTS

Special thanks to the Bundesministerium für Wirtschaft (BMWi) and AiF for their financial support in the ZIM project BIATO. Thanks to the project partners SIOS Meßtechnik GmbH Ilmenau and Lehren- und Messgerätewerk (LMW) GmbH Schmalkalden for their comprehensive support.

8. REFERENCES

[1] Kühnel M, Ullmann V, Gerhardt U, Manske E, 2012, Automated Setup for non-tactile high-precision measurements of roundness and cylindricity using two laser interferometers *Meas. Sci. Technol.* **23** 074016

[2] Ullmann V, Kühnel M, Gerhardt U, Manske E, 2011, Metrological Traceable Interferometrical Measurement of Circle and Cylinder Form Deviations on Ring Gauges *MacroScale 2011 (Bern, Oktober 2011)*

[3] Manske E, Jäger G, Schmidt I, Pöschel W and Kühnel M, 2007, High-precision estimation of circle and cylinder form deviations by means of a fibre-coupled laser interferometer arrangement *Proc. of the 7th Int. Conf. european society for precision engineering and nanometrology* (*Bremen, D, May 2007*)

[4] Meli F and Küng A, 2007, AFM investigation on surface damage caused by mechanical probing with small ruby spheres *Meas. Sci. Technol.* **18** 496-502

[5] Zahurska O, 2014, Rechnergestützte Verarbeitung und Auswertung von Messdaten in der interferenzoptischen Formmesstechnik, *TU Ilmenau*: 34-36

[6] DIN EN ISO 12181-2, 07-2009, Geometrische Produktspezifikation (GPS) – Rundheit – Teil 2: Spezifikationsoperatoren (ISO/DIS 12181-2:2009) – Entwurf –, *Normenausschuss Technische Grundlagen (NATG) im DIN*: 5-8

[7] VDI/VDE 2631, 08-2007, Form measurement – characteristics and selection of filters, *VDI/VDE-Gesellschaft Mess- und Automatisierungstechnik (GMA), Fachausschuss Formprüfung*: 7-10

[8] Bronstein et.al., *Taschenbuch der Mathematik*, Wissenschaftlicher Verlag Harry Deutsch GmbH, Frankfurt am Main, 7.Aufl., 2008: 998-999

[9] Donaldson R R, 1972, A simple method for separating spindle error from test ball roundness error *CIRP Annals* **21**(1): 125-126

[10] Tan J-B, Li D-S, Qiang X-F, Zhao X-P, Yang W-G, 1993, Error separation technique of “two points and two settings method” and application in contactless automatic measurement *SPIE Vol. 2101 Measurement Technology and Intelligent Instruments*

CONTACTS

M.Sc. Vinzenz Ullmann vinzenz.ullmann@tu-ilmenau.de
Dr.-Ing. Michael Kühnel michael.kühnel@tu-ilmenau.de
Prof. Dr.-Ing. habil. E. Manske eberhard.manske@tu-ilmenau.de